J. Appl. Math. & Informatics Vol. **35***(2017), No. 3 - 4, pp. 241 - 260*
https://doi.org/10.14317/jami.2017.241

EFFECT OF FLOW UNSTEADINESS ON DISPERSION IN NON-NEWTONIAN FLUID IN AN ANNULUS

P. NAGARANI* AND B.T. SEBASTIAN

Abstract. An analysis is made to study the solute transport in a Casson fluid flow through an annulus in presence of oscillatory flow field and determine how this flow influence the solute dispersion along the annular region. Axial dispersion coefficient and the mean concentration expressions are calculated using the generalized dispersion model. Dispersion coefficient in oscillatory flow is found to be a function of frequency parameter, Schmidt number, and the pressure fluctuation component besides its dependency on yield stress of the fluid, annular gap and time in the case of steady flow. Due to the oscillatory nature of the flow, the dispersion coefficient changes cyclically and the amplitude and magnitude of the dispersion increases initially with time and reaches a non - transient state after a certain critical time. This critical value varies with frequency parameter and independent of the other parameters. It is found that the presence of inner cylinder and increase in the size of the inner cylinder inhibits the dispersion process. This model may be used in understanding the dispersion phenomenon in cardiovascular flows and in particular in catheterized arteries.

AMS Mathematics Subject Classification : 65H05, 65F10.
Key words and phrases : Convection-diffusion; Longitudinal Dispersion; Generalized dispersion model; Oscillatory flow; Non-Newtonian fluids; Catheterized artery.

1. Introduction

The flow/dispersion in tube/annulus has abundant applications in different branches of engineering, chemical processing industries, biomechanics and petroleum science. The problems of mass transfer have been used for the construction of high-performance liquid chromatography instruments to analyse the effective diffusivity of liquids [12]. The annular chromatographic method is used for separation of metals, sugars and proteins [6, 9, 16] . In the indicator dilution technique, it is a common practice among physiologists to use catheters

Received June 11, 2016. Revised January 9, 2017. Accepted February 13, 2017. *Corresponding author.

to inject the dye and to withdraw blood samples for the purpose of measurements [4, 14, 32]. The study of the blood-tissue exchange is also done using the multiple dilution technique which often needs frequent sampling of the blood using of catheters [34].

Due to wide range of applications of dispersion phenomenon, several researchers studied the dispersion in Newtonian/non-Newtonian fluids. The very well known analyses used in these studies are due to Taylor [35], Aris [1] and the derivative expansion method (also known as generalized dispersion model) given by Gill and Sankarasubramanian [18]. Aris [2] studied the dispersion of a solute in coaxial annular region by considering two phases in which the solute can also pass into another fluid phase flowing in an annular region around the first. This study illustrates the applications of the model in distillation and partition chromatography. Using generalized dispersion model, Rao and Deshikachar [31] studied the dispersion problem in annuls in the case of Newtonian fluid and this theory was extended by Sarkar and Jayaraman [32] in the case of wall absorption. Ramana and Sarojamma [30] studied the dispersion of a solute in an annulus considering the flowing fluid as Herschel - Bulkley by using the generalized dispersion model.

The oscillatory flow models have gained attention due to its applications in industry, environment, estuaries, modelling of transport phenomena in cardiovascular flows and in understanding the exchange of mass and heat between the lung and environment [21]. Aris [3] studied the dispersion phenomenon in oscillatory flow filed using his method of moments. In view of the applications of the dispersion in estuaries, Chatwin [11] studied the dispersion of a passive contaminant in a tube in which the flow is driven by a longitudinal pressure gradient varying harmonically with time. Tsangaris and Athanassiadis [36] obtained the effective diffusion coefficient of a contaminant in an oscillatory flow in annulus by considering the flowing fluid as Newtonian. Pedley and Kamm [29] studied the axial dispersion in an annulus in a curved tube in the presence of oscillatory flow filed by asymptotic analysis for the limiting case of small annular gap and by numerical solution for arbitrary annular gap. Hydon and Pedley [20] analysed the axial dispersion in a finite channel with oscillating walls and in presence of oscillating flow to application of the axial dispersion to understand the gas transport in the airways of the lung. Using, generalized dispersion model the dispersion problem in oscillatory flows in Newtonian fluid with conductive walls was studied by Jiang and Grotberg [21].The annulus problem with wall absorption is studied by Sarkar and Jayaraman [33] and discussed the application of the models to the catheterized artery.

Blood flow in arteries shows various properties such as pulsatility, curvature, branching, and elastic walls and the transport of any species in the blood is affected by these phenomena. Blood flow is pulsatile in nature with the same

frequency as the heartbeat. The experimental data on blood properties [13] showed that for small shear rate ($\dot{\gamma} < 10\ s^{-1}$) and for hematocrit less than 40% the properties of blood can be described approximately by Casson's equation. Experiments on blood also revealed that blood has a finite yield stress of 0.04 $dynes/cm^2$ at 40% hematocrit [13] . Also, various experiments conducted on blood [10, 23, 24, 25] with different heamatocrits, anticoagulants and temperature confirmed that the flow of blood can be described by Casson's fluid model over a wide range of shear rates, say (1-100,000 s^{-1}), and more accurately at low shear rates ($\dot{\gamma} < 20\ s^{-1}$). Hence, the modification to the classical Taylor-Aris and Gill-Sankarasubramanian's dispersion theory caused by pulsatility and non-Newtonian rheology is very important to analyse the dispersion in blood flows. In these directions, Nagarani et al. [27] studied the effects of boundary absorption on dispersion in Casson fluid flow in an annulus in the case of steady flow. They showed that an increase in yield stress and decrease in annular gap, decreases the dispersion coefficient.

With this primary motive to understand the combined effects of the flow oscillation, annular gap and the Non-Newtonian rheology on dispersion process here we gave a mathematical model of dispersion of a solute in Casson fluid flow in an annulus in presence of oscillatory flow. We used the generalized dispersion model to study the process and according to this modal the whole process is expressed in terms of convection and dispersion coefficients. The expression for mean concentration is obtained. Pictorial representations of the mean concentration and dispersion coefficient for the variation of other parameters are shown in section 4. Results are discussed and interpreted with physical significance of the observed variations. Application of this study in understanding the dispersion process in a catheterized artery is discussed in section 5.

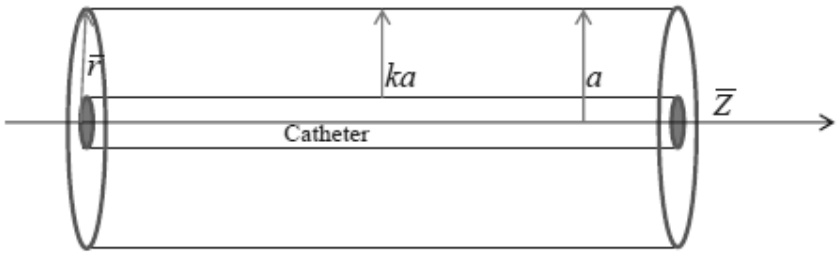

FIGURE 1. Schematic diagram of the proposed model

2. Mathematical Formulation

We considered an unsteady, axi-symmetric, incompressible, pulsatile flow of a Casson fluid flowing in an annulus. Here the annulus is considered to be formed between two coaxial cylinders whose inner cylinder radius is ka $(0 < k < 1)$ and the outer cylinder radius is a. The axial and radial coordinates are represented by $\bar{z}$ and $\bar{r}$, respectively (Fig.1). The dispersion of a bolus of solute, which is initially of $\bar{z}_s$ units in length and of uniform concentration C_0 is studied. For fully developed axisymmetric incompressible flow, the unsteady convective diffusion equation which describes the local concentration $C\ (t,\ z,\ r)$ of a solute in non-dimensional form can be written as,

$$\frac{\partial C}{\partial t} \ + \ w(t,r)\,\frac{\partial C}{\partial z} \ = \ \left(\frac{1}{r}\,\frac{\partial}{\partial r}\,(\,r\,\frac{\partial}{\partial r}\,) \ + \ \frac{1}{Pe^2}\,\frac{\partial^2}{\partial z^2}\right) C. \tag{1}$$

with non-dimensional quantities

$$C = \frac{\bar{C}}{C_0},\ \ z = \frac{D_m \bar{z}}{a^2 w_0},\ \ t = \frac{D_m \bar{t}}{a^2}, r = \frac{\bar{r}}{a}, w = \frac{\bar{w}}{w_0}. \tag{2}$$

Where t is the time, w is the axial velocity, D_m is the coefficient of molecular diffusion, which is assumed to be a constant, $w_0 = \frac{P_0 a^2}{2\mu_\infty}$, μ_∞ is the Newtonian viscosity of the fluid, P_0 is the steady state component of pressure gradient of the fluid, $Pe = \frac{a w_0}{D_m}$, the Peclet number and k is the non-dimensional radius of the inner cylinder (also the ratio of inner cylinder to outer cylinder radius). The variables with bar represent the corresponding dimensional quantities.

The initial condition considered can be written in non-dimensional form as

$$C\,(0\,,z,\,r\,) \ = \begin{cases} 1\,, & |z| \ \leq \ \frac{z_s}{2} \\ 0\,, & |z| \ > \ \frac{z_s}{2} \end{cases} \tag{3}$$

and the boundary conditions in dimensionless form for the given model are

$$\frac{\partial C}{\partial r}(t,\ z,\ k) \ = 0 \tag{4a}$$

$$\frac{\partial C}{\partial r}\,(t,\ z,\ 1) \ = 0 \tag{4b}$$

Conditions (4a) and (4b) constitute the non-flux condition at the impermeable walls of the inner tube $(r = k)$ and outer tube $(r = 1)$ respectively. Since the amount of solute in the system is finite we also will have,

$$C\,(\,t\,,\ \infty\,,\ r) \ = \ 0. \tag{5}$$

2.1. Casson's Constitutive Equation and Velocity distribution in an annulus. The constitutive equation for a Casson fluid relating the stress (τ) and shear rate $\frac{\partial w}{\partial r}$ in non-dimensional form is given by

$$\tau^{\frac{1}{2}} = \tau_y^{\frac{1}{2}} + \left(-\frac{\partial w}{\partial r}\right)^{\frac{1}{2}} \ \text{if } \tau \geqslant \tau_y \tag{6a}$$

$$\frac{\partial w}{\partial r} = 0 \qquad \text{if } \tau \leqslant \tau_y \tag{6b}$$

where $\tau = \frac{\bar{\tau}}{\mu_\infty (w_0/a)}$ and $\tau_y = \frac{\bar{\tau}_y}{\mu_\infty (w_0/a)}$ are the non-dimensional shear stress and yield stress respectively. The relation given above in (6a-b) is appropriate for the case when τ is positive and $\frac{\partial w}{\partial r}$ is negative. The more general situation where τ and $\frac{\partial w}{\partial r}$ can change the sign (in the case of annular flow as Bird et al., [5]) and can be written as,

$$\frac{\partial w}{\partial r} = -\left[1 + \frac{\tau_y}{|\tau|} - 2\frac{\tau_y^{1/2}}{|\tau|^{1/2}}\right]\tau \qquad \text{if } |\tau| \geq \tau_y \tag{7a}$$

$$\frac{\partial w}{\partial r} = 0 \qquad \text{if } |\tau| \leq \tau_y \tag{7b}$$

From Eqs. (7a) and (7b), we can see that the flow of a Casson fluid in an annulus has three phases such as that in the central region velocity profile is flat and, hence, forms a plug flow region. In the plug flow region the fluid does not flow by itself, but is carried along by the fluid in the two adjacent shear flow regions as a solid body with a constant velocity, which is known as the plug flow velocity. If the plug flow region is represented by $\lambda_1 \leq r \leq \lambda_2$ $(k \leq \lambda_1,\ \lambda_2 \leq 1)$ then the two shear flow regions can be represented as $k \leq r \leq \lambda_1$ and $\lambda_2 \leq r \leq 1$. Here λ_1 and λ_2 are known as yield plane locations. Then the Casson constitutive Eq.(7) in these regions can be written as,

$$\frac{\partial w}{\partial r} = -\tau + \tau_y - 2\tau_y^{1/2}|\tau|^{1/2} \quad \text{if } k \leq r \leq \lambda_1 \tag{8a}$$

$$\frac{\partial w}{\partial r} = 0 \qquad \text{if } \lambda_1 \leq r \leq \lambda_2 \tag{8b}$$

$$\frac{\partial w}{\partial r} = -(\tau + \tau_y - 2\tau_y^{1/2}\tau^{1/2}) \qquad \text{if } \lambda_2 \leq r \leq 1 \tag{8c}$$

The velocity expression for the case of pulsatile flow in Casson fluid flow in these regions is given by Dash et al. [14] as

$$w(t,r) = w^+(r,t) = \frac{\partial p}{\partial z}(t)\left[\lambda^2 \ln(r/k) - \left(\frac{r^2-k^2}{2}\right) + \Omega\,(r-k) - 2\Omega^{1/2}\int_k^r \left(\frac{\lambda^2 - r^2}{r}\right)^{1/2} dr\right] \qquad \text{for } k \leq r \leq \lambda_1 \tag{9a}$$

$$w(t) = w^- = w_p = w^+(t,\lambda_1) = w^{++}(t,\lambda_2) \qquad \text{for} \quad \lambda_1 \leq r \leq \lambda_2 \tag{9b}$$

$$w(t,r) = w^{++}(r,t) = \frac{\partial p}{\partial z}(t)\left[\lambda^2 \ln(r) + \left(\frac{1-r^2}{2}\right) + \Omega(1-r) - 2\Omega^{1/2}\int_r^1 \left(\frac{r^2 - \lambda^2}{r}\right)^{1/2} dr\right] \qquad \text{for } \lambda_2 \leq r \leq 1 \tag{9c}$$

where

$$\lambda^2 = \lambda_1 \lambda_2 \tag{10a}$$

$$\Omega = \lambda_2 - \lambda_1 = \frac{\tau_y}{\frac{\partial p}{\partial z}(t)} \tag{10b}$$

is the width of the plug region. The superscripts "+" and "++" represent the shear flow regions $k \leq r \leq \lambda_1$ and $\lambda_2 \leq r \leq 1$, respectively, and the superscript "–" represents the plug flow region $\lambda_1 \leq r \leq \lambda_2$. Also,

$$\frac{\partial p}{\partial z}(t) = 1 + e \cos \alpha^2 Sct, \tag{11}$$

where, $e = \frac{P_1}{P_0}$ is the amplitude of the pulsatile pressure gradient, $\alpha = a\sqrt{\frac{\omega}{\nu}}$ is the Womersley number, $Sc = \frac{\upsilon}{D_m}$ is the Schmidt number, P_1 is the fluctuating component of pressure, ω is the frequency of pressure pulsation, ν is the kinematic viscosity. Here the product $\alpha^2 Sc$ is a measure of the ratio of the characteristic time of transverse diffusion to the period of oscillation since $\alpha^2 Sc$ can be taken as

$$\alpha^2 Sc = \left(\frac{a^2\omega}{\nu}\right)\left(\frac{\nu}{D_m}\right) = \frac{(a^2/D_m)}{(1/\omega)} = \frac{t_1}{t_2} \tag{12}$$

where the time for lateral transport of mass is t_1 and period of oscillation t_2. From the continuity condition of velocity distribution (9a) and (9b), λ_1 must satisfies the equation

$$3\Omega^2 + 6\Omega\lambda_1 - 2\lambda_1(\lambda_1 + \Omega)\,\ln\left[k(\lambda_1 + \Omega)/\lambda_1\right] - (1+k)(2\Omega + 1 - k) -$$
$$4\Omega^{1/2}\left[\int_k^{\lambda_1}\left(\frac{\lambda_1(\lambda_1+\Omega) - r^2}{r}\right)^{1/2} dr \; - \int_{\lambda_1+\Omega}^{1}\left(\frac{r^2 - \lambda_1(\lambda_1+\Omega)}{r}\right)^{1/2} dr\right] = 0 \tag{13}$$

This integral equation is solved numerically for λ_1 using the Regular - Falsi method. Once is known λ_2 can be obtained from (10a) and (10b).

3. Method of Solution

The solution of the convective-diffusion equation (1) along with the given set of initial and boundary conditions (3)-(5) by following the analysis of Gill and Sankarasubramanian [18] can be assumed as

$$C = C_m + \sum_{i=1}^{\infty} f_i(t, r)\,\frac{\partial^i C_m}{\partial z^i} \tag{14}$$

where the dimensionless mean concentration C_m is defined as

$$C_m \;=\; \frac{2}{1-k^2}\;\int_k^1 C\, r\, dr. \tag{15}$$

Multiplying Eq.(1) by $\frac{2r}{1-k^2}$ and integrating with respect to r from k to 1, we get

$$\frac{\partial C_m}{\partial t} = \frac{1}{Pe^2}\frac{\partial^2 C_m}{\partial z^2} - \frac{2}{1-k^2}\frac{\partial}{\partial z}\int_k^1 w(t,r)\,C(t,z,r)\,r\,dr\,. \tag{16}$$

If we introduce (14) into (16), the dispersion model for C_m, by assuming the process of distributing C_m is diffusive in nature right from the time is zero, is obtained as

$$\frac{\partial C_m}{\partial t} = \sum_{i=1}^{\infty} K_i(t)\frac{\partial^i C_m}{\partial z^i}, \tag{17}$$

where

$$K_i(t) = \frac{\delta_{i2}}{Pe^2} - \frac{2}{1-k^2}\int_k^1 f_{i-1}\,(t,r)\,w(t,r)\,r\,dr, \qquad \text{i} = 1,\, 2..... \tag{18}$$

and δ_{ij} denotes Kronecker delta,

$$\delta_{ij} = \begin{cases} 1, & i = j \\ 0, & i \neq j. \end{cases} \tag{19}$$

Here K_1 and K_2 are termed as convection and dispersion coefficients respectively for C_m. Using (14), (17) in (1) and equating the coefficients of $\frac{\partial^n C_m}{\partial z^n}$, $n = 1, 2\ldots$ the set of differential equations for f_n are obtained as

$$\frac{\partial f_n}{\partial t} = \frac{1}{r}\frac{\partial}{\partial r}(r\frac{\partial f_n}{\partial r}) - w(t,r)f_{n-1} + \frac{1}{Pe^2}f_{n-2} - \sum_{i=1}^{n} K_i f_{n-i}, \qquad n = 1, 2, \ldots \tag{20}$$

The initial and boundary conditions for f_n are obtained from (3)-(5) as

$$f_n(0,r) = 0, \qquad n = 1, 2, \ldots \tag{21}$$

$$\frac{\partial f_n}{\partial r}(t,k) = 0, \qquad n = 1, 2, \ldots \tag{22a}$$

$$\frac{\partial f_n}{\partial r}(t,1) = 0, \qquad n = 1, 2, \ldots \tag{22b}$$

Since Eqs. (18) and (20) are coupled, we solved these equations one after the other. From Eq.(18), the expression for $K_1(t)$ is obtained as

$$K_1 = \frac{-2}{1-k^2}\int_k^1 w(t,r) r\,dr. \tag{23}$$

The analytical expression for K_1 is obtained but not provided since the expression is cumbersome. The equation for f_1 from (20) can be written as

$$\frac{1}{r}\frac{\partial}{\partial r}(r\frac{\partial f_1}{\partial r}) - \frac{\partial f_1}{\partial t} = K_1(t) + w(t,r) \tag{24}$$

and the initial and boundary conditions for f_1 from Eqs. (21) and (22) are

$$f_1(0,r) = 0 \tag{25a}$$

$$\frac{\partial f_1}{\partial r}(t,k) = 0 \tag{25b}$$

$$\frac{\partial f_1}{\partial r}(t,1) = 0 \tag{25c}$$

The solution of the non-homogeneous boundary value problem (24) subjected to the conditions (25a-c) is obtained as [7] ,

$$\begin{aligned} f_1(t,r) &= \sum_{n=1}^{\infty} \left[\frac{\int_0^t e^{-\mu_n^2(t-s)} \gamma_n(s) ds \, E_0(\mu_n r)}{\int_k^1 r E_0^2(\mu_n r) dr} \right] \\ &= \left[\sum_{n=1}^{\infty} \frac{2}{E_0^2(\mu_n) - k^2 E_0^2(\mu_n k)} \int_0^t e^{-\mu_n^2(t-s)} \gamma_n(s) ds \, E_0(\mu_n r) \right] \end{aligned} \tag{26}$$

where γ_n are given by

$$\gamma_n(s) = -\int_k^1 \left[w(t,r) + K_1(t) \right] r E_0(\mu_n r) \, dr \tag{27a}$$

$$E_0(\mu_n r) = Y_0(\mu_n r) J_1(\mu_n) - J_0(\mu_n r) Y_1(\mu_n) \tag{27b}$$

μ_n are the roots of the equation

$$Y_1(\mu_n k) J_1(\mu_n) - J_1(\mu_n k) Y_1(\mu_n) = 0. \tag{27c}$$

J_0 and J_1 are Bessel functions of first kind of order zero and one, respectively, and Y_0 and Y_1 are Bessel functions of second kind of order zero and one, respectively. The dispersion coefficient can be obtained using (18), (26) and (27a-c) as

$$K_2 - \frac{1}{Pe^2} \;=\; -\frac{2}{1-k^2} \int_0^1 w(t,\, r) \; f_1(t,\, r)\, r \; dr. \tag{28}$$

We calculated K_2 numerically since the expressions for $w(t,r)$ and $f_1(t,r)$ are cumbersome. By neglecting the terms that involved K_3, K_4 etc., in Eq.(18) the generalized dispersion model takes the form

$$\frac{\partial C_m}{\partial t} = \; K_1(t) \, \frac{\partial C_m}{\partial z} \; + \; K_2(t) \, \frac{\partial^2 C_m}{\partial z^2}. \tag{29}$$

The initial and boundary conditions for $C_m$are obtained as

$$C_m(0,z) = \begin{cases} 1 & \text{if } |z| \leqslant \frac{z_s}{2} \\ 0 & \text{if } |z| > \frac{z_s}{2} \end{cases} \tag{30}$$

$$C_m(t,\, \infty) = \; 0. \tag{31}$$

The mean concentration C_m from Eq. (29) satisfying conditions (30) and (31) can be obtained as

$$C_m = \frac{1}{2} \left[erf \left[\frac{\frac{1}{2} z_s + z_1}{2 z_2^{\frac{1}{2}}} \right] + erf \left[\frac{\frac{1}{2} z_s - z_1}{2 z_2^{\frac{1}{2}}} \right] \right], \tag{32}$$

where

$$z_1 = z + \int_0^t K_1(\eta)\ d\eta \tag{33a}$$

$$z_2 = \int_0^t K_2(\eta)\, d\eta. \tag{33b}$$

4. Results and Discussion

Present study analyses the effects of flow oscillation, annular gap and yield stress of the fluid on the dispersion process. It is observed that dispersion coefficient in oscillatory flow is a function of Womersely frequency parameter α, Schmidt number Sc and fluctuating pressure component e in addition to its dependency on the dispersion time t, yield stress of the fluid τ_y and the radius of the inner cylinder k (or in other words annular gap) in case of steady flow problem. The mean concentration C_m is also a function of the above parameters, and in addition the slug input length z_s. In the present discussion, we fixed both Pe and Sc at 1000, the frequency parameter α is considered as small (< 1), the range 0-0.2 is taken for τ_y, the range 0.1-0.3 is taken for k, the fluctuating component e is taken from 0 to 0.5 and z_s is taken 0.02 and 0.004. These ranges of values were chosen as these are typical ranges in the cardiovascular system. For each value of k, the yield plane locations are found numerically from Eqs.(10) and (13). For each value of k, the associated eigenvalues μ_n for $n = 1, 2 \ldots$ are calculated numerically using Eq. (27c). The results reduced to the steady case when $e = 0$ and to the Newtonian case when $\tau_y = 0$. The results show good agreement with Dash et al. [15] with steady case and $k \to 0$, and with Gill and Sankarasubramanian [18] in the limit case as $k \to 0$ and in Newtonian steady case.

Figures 2-5, project the variation of dispersion coefficient K_2 (from which the additive contribution of the $1/Pe^2$ is deducted) with time t for different values of τ_y, k, e and α by fixing $Sc = 1000$. It can be seen from Eqs.(9) –(12), that the velocity of the fluid is periodic with period $T_L = \frac{2\pi}{\alpha^2 Sc}$ and hence for $\alpha = 0.05$, 0.1 and 0.2 the time periods are 2.5, 0.628 and 0.157, respectively for $Sc = 1000$. Figs. 2-5 show the results for four cycles for the variation of dispersion coefficient with time t for the variation of other parameters. It is observed that due to the oscillatory nature of the flow the dispersion coefficient changes cyclically and the amplitude and magnitude of the dispersion increases initially with time and reaches a non-transient state after a certain critical time. This critical value of this time varies with α and independent of τ_y, e and k. It is observed that as τ_y increases the amplitude of the fluctuations of K_2 decreases and also decreases the magnitude of the dispersion coefficient. This nature is expected as an increase in τ_y results in a decrease in the flow velocity, and hence the dispersion rate.

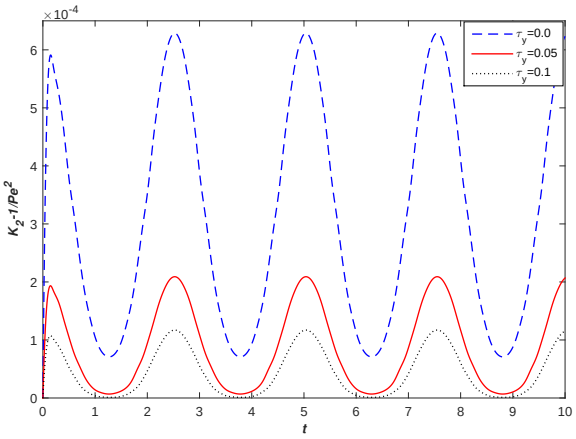

(a)

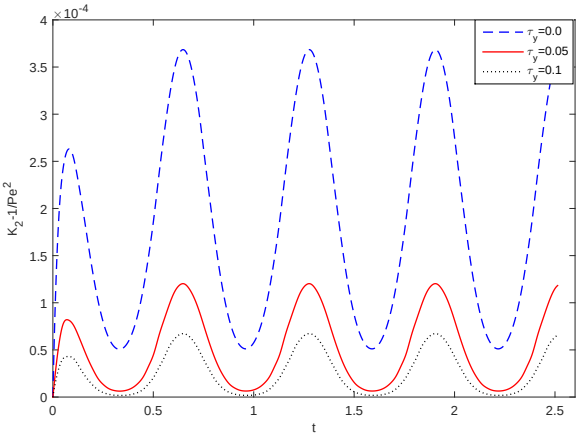

(b)

FIGURE 2. Variation of dispersion coefficient $(K_2 - 1/Pe^2)$ with t for different, values of τ_y when $e = 0.5$, $k = 0.1$ a) $\alpha = 0.05$ b) $\alpha = 0.1$

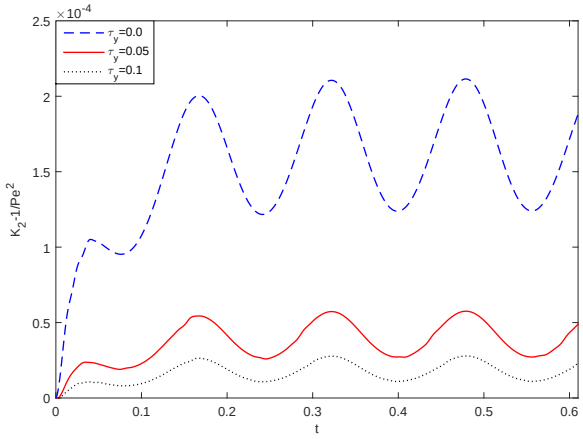

(a)

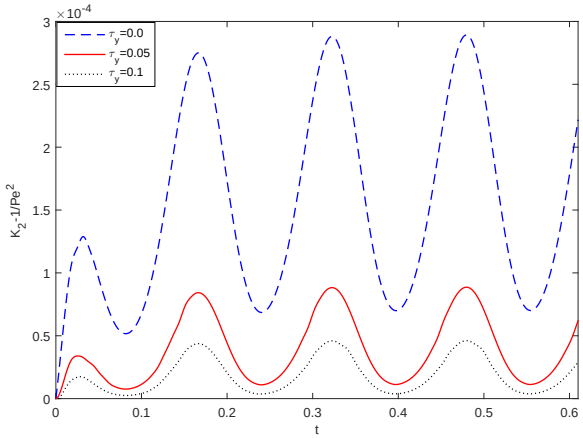

(b)

FIGURE 3. Variation of dispersion coefficient $(K_2 - 1/Pe^2)$ with t for different values τ_y $when$ $\alpha = 0.2, k = 0.1$ $a)$ $e = 0.2$ $b)$ $e = 0.5$

From Figs.2 (a-b) it is observed that the critical time to reach non-transient state is different for different α. For $\alpha = 0.05$ that critical time is about $t = 2.5$, but for $\alpha = 0.1$ it is about 0.55 when $k = 0.1$, $e = 0.5$ and for all τ_y We could see from Figs. 2 (a-b) that the magnitude of K_2 decreases with α, which could be due to an increase in α which decreases the flow, and hence reduces K_2. Also, the amplitude of fluctuations of K_2 increases with α. The maximum amplitude of K_2 is 2.089×10^{-4} at $\alpha = 0.05$ and 1.185×10^{-4} at $\alpha = 0.1$ in the case of non-Newtonian fluid ($\tau_y = 0.05$). Also in the case of Newtonian fluid ($\tau_y = 0$) it is seen that the maximum value of K_2 is changing from 6.273×10^{-4} to 3.683×10^{-4}

as α changes from 0.05 to 0.1.

Figures 3 (a-b) show the variation of K_2 with e and we can notice that as e increases the fluctuations and the magnitude of K_2 increases. Also the value of K_2 is changing from 5.719×10^{-5} to 8.739×10^{-5} when e changes from 0.2 to 0.5 for $\alpha = 0.2$ in the case of non-Newtonian fluid ($\tau_y = 0.05$). Fig. 4 compares the results of the variation of dispersion coefficient in the case of different e and one can observe from the figure as e increases the peak value of the dispersion coefficient also increases. Fig. 5 shows variation of dispersion coefficient explic-

itly for different k values in the case of Casson fluid ($\tau_y = 0.05$) by fixing the other parameters. It is noticed that the decrease in the annular gap inhibits the dispersion process which could be due to decrease in annular gap leads to decrease of flow in the annulus, which causes the lower mass transfer rate, as was noticed by Rao and Desikachar [33] . It is seen that the dispersion coefficient decreases from 5.719×10^{-5} to 3.704×10^{-6} as k increases from 0.1 to 0.3 at time $t = 0.1$, when $\tau_y = 0.05$.

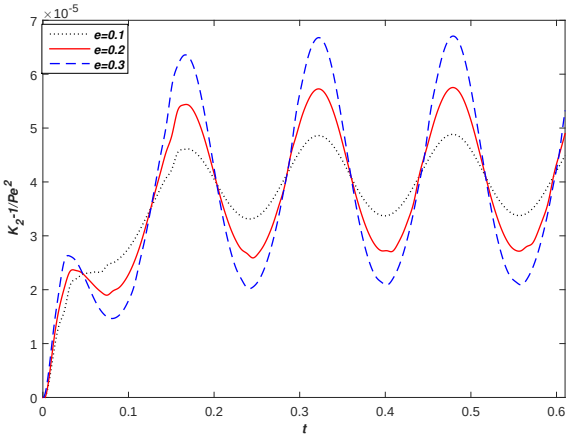

FIGURE 4. Variation of dispersion coefficient ($K_2 - 1/Pe^2$) with t for different values of e when $\tau_y = 0.05$, $\alpha = 0.2$, $k = 0.1$

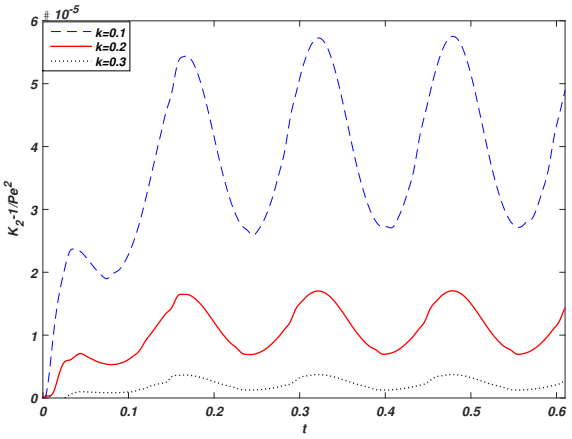

FIGURE 5. Variation of dispersion coefficient $(K_2 - 1/Pe^2)$ with t for different values of k when $e = 0.5$, $\alpha = 0.2$,, $\tau_y = 0.05$

Figures 6-11 show the variation of mean concentration C_m for oscillatory flow with axial distance z for the variation of t, τ_y, z_s, α, e and k. Figs. 6 (a-b) show the variation of C_m with τ_y for $\alpha = 0.05$ and 0.1, respectively. In both the cases, it is seen that the peak value of mean concentration increases with τ_y, which matches with earlier results of Dash et al. [15] . Fig. 7 depicts the variation of mean concentration C_m with α. We noticed that as α increases the peak of the mean concentration increases, and also C_m decays faster for larger α. It is also noticed that when α changes from 0.05 to 0.1 the change in mean concentration is more as compared to changing α from 0.1 to 0.2.Fig. 8 shows the variation of C_m for different values of e and one can observe that as e increases the peak of the mean concentration decreases and also observed that as e increases the peak of C_m shifts towards right. Fig. 9 shows the variation of C_m for different values of k. It is seen that as k increases the peak of the mean concentration increases and shifts towards the left. The peak value of C_m in the case of Non-Newtonian fluid ($\tau_y = 0.05$) increases from 0.8217 to 0.9998 as k increases from 0.1 to 0.3 (Fig. 9). Fig. 10 shows the variation of C_m with z for the variation of the initial slug input of solute length z_s. It is observed that the values of C_m is less in magnitude in the case z_s= 0.004 and other properties are similar as in all the three cases when z_s= 0.004, 0.008 and 0.02. We also see that as t increases the peak of mean concentration decreases (Fig. 12), which shows that as time progress the concentration of the solute decreases.

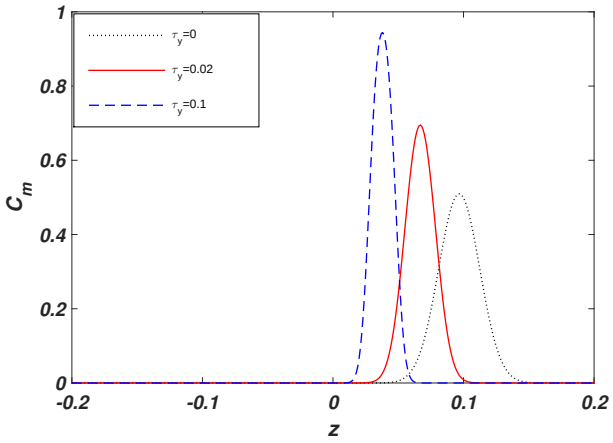

(a)

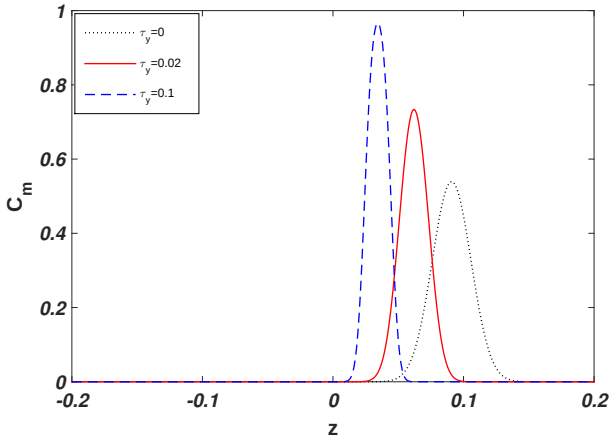

(b)

FIGURE 6. Axial distribution of mean concentration C_m different τ_y when e = 0.1, z_s = 0.02, k = 0.1 a) α= 0.05 b) α= 0.1

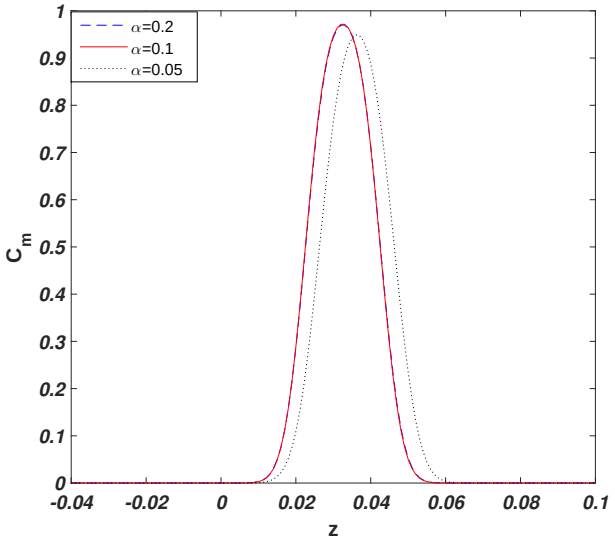

FIGURE 7. Axial distribution of mean concentration C_m different α when $e = 0.1$, $t = 0.1$, $z_s = 0.02$, $k = 0.1$, τ_y=0.1

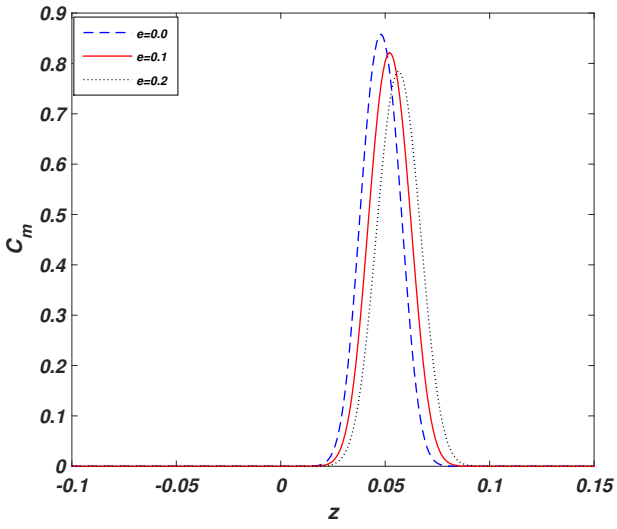

FIGURE 8. Axial distribution of mean concentration C_m different e when τ_y= 0.05 z_s= 0.02, $k = 0.1$, $\alpha = 0.05$

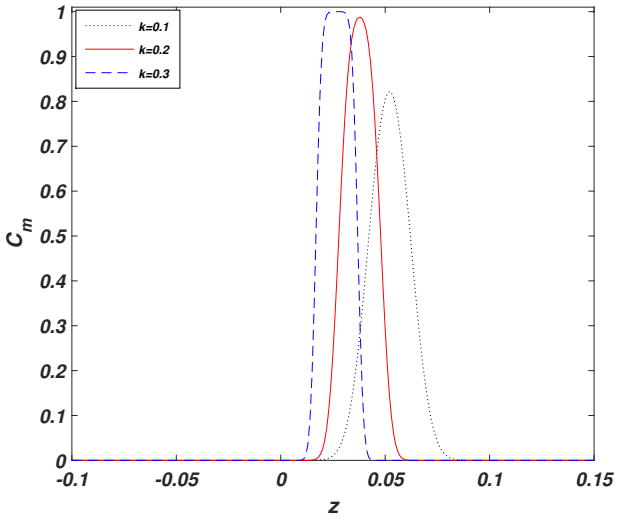

FIGURE 9. Axial distribution of mean concentration C_m different k when $e = 0.1$ $z_s = 0.02$, $k = 0.1$, $\alpha = 0.05$, $\tau_y = 0.05$

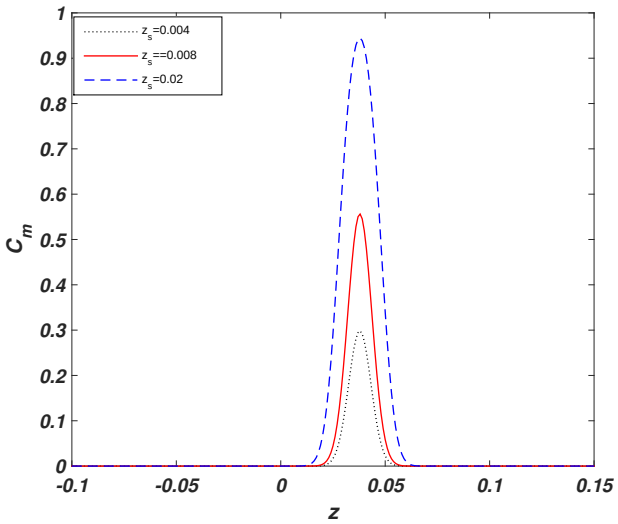

FIGURE 10. Axial distribution of mean concentration C_m for different z_s when $e = 0.1$, $\tau_y = 0.1$, $k = 0.1$, $\alpha = 0.05$

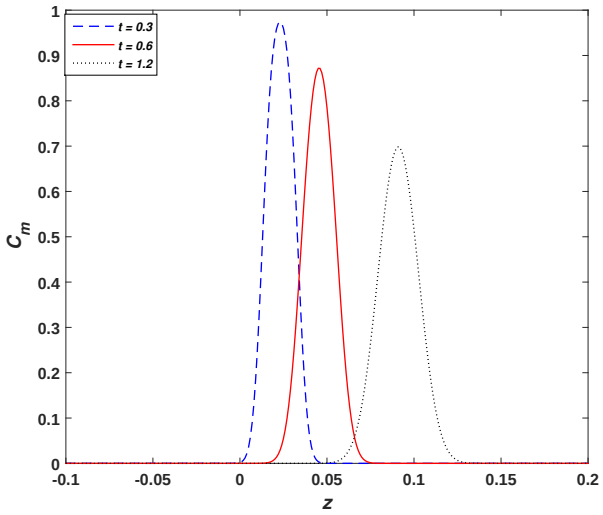

FIGURE 11. Axial distribution of mean concentration C_m different t , when e = 0.1, τ_y = 0.05, z_s= 0.02, k= 0.1, α = 0.1

5. Application to Catheterized Artery

The mathematical model presented in Sections 2 and 3 can be used to understand the dispersion of an indicator in a catheterized artery of radius a and the catheter radius ka, $(0 < k < 1)$ which is introduced coaxially. We considered the flow is oscillatory since the blood flow is unsteady owing to the pumping of the heart and also the flowing fluid as Casson fluid to account for the yield stress of the blood [17, 22]. The objective of the model is to provide the correction for the catheter induced errors in the measured values based on axial dispersion of substance owing to combined action of convection and diffusion. The introduction of a catheter into the blood vessel can be potent cause of eddy formation and mixing of blood. The introduction of catheter always introduces some distortion in the time concentration curve so that recorded curve is not of the same shape as the *in situ* concentration - time relation at the withdrawal site [26] . Experimental studies with calibration based on mathematical models for the removal of the catheter distortion are reported in [19, 28] . The ratio of catheter size to radius of the artery is taken in the range of 0.1 to 0.3 to analyse the effect of catheter size on the transport process. The values of the yield stress are varied from 0 to 0.1; the Womersley frequency parameter (α) is taken as $<$ 1 and the value of Schmidt is fixed at 1000, so that the results can be applied to cardiovascular flows [8] .

The discussion in the Section 4 shows that the catheter size and yield stress have an effect on dispersion coefficient in catheterized arteries. The variation of

K_2 with catheter size k for different values of τ_y is illustrated in Table 1. The tabulated values show that the presence of the catheter decreases the dispersion coefficient and also increase in the size of catheter further decreases the dispersion coefficient in both Newtonian ($\tau_y = 0$) and non-Newtonian ($\tau_y \neq 0$) cases. In the case of Newtonian fluid, the insertion of catheter of size 0.1 in a normal artery decreases the dispersion coefficient by 79% where as in the case of Casson fluid ($\tau_y = 0.05$) this decrease is 88%. The effect of yield stress is seen to decrease the dispersion coefficient in both the normal artery as well as the catheterized artery. In the case of normal artery ($k = 0$) the decrease in dispersion coefficient is 98% when τ_y increases from 0 (Newtonian) to 0.05 (Casson), where in the case of catheterized artery (size 0.1) the decrease in dispersion coefficient is 80%. Hence, one can see that the combined influence of both non-Newtonian nature and presence of the catheter significantly inhibits the dispersion process. We see that an increase in the frequency parameter helps the dispersion of the dye. The axial variation of concentration for the variation of other parameters is discussed through Figs. 6 – 11, which provides the understanding of dispersion of the dye along the axial direction, which is very much essential.

	$\tau_y = 0$	$\tau_y = 0.02$	$\tau_y = 0.05$
$k = 0.0$	9.539×10^{-4}	4.017×10^{-4}	2.145×10^{-4}
$k = 0.1$	1.980×10^{-4}	4.847×10^{-5}	2.476×10^{-5}
$k = 0.2$	4.117×10^{-5}	1.451×10^{-5}	6.715×10^{-6}
$k = 0.3$	1.277×10^{-5}	3.314×10^{-6}	1.097×10^{-6}

Table 1. Variation of dispersion coefficient K_2 with k and τ_y when $\alpha = 0.05$, $e = 0.2, t = 1$

6. Conclusion

Dispersion of solute in an annulus in oscillatory flow with flowing fluid is modelled as Casson fluid is studied using the generalized dispersion model. It is found that the dispersion coefficient in oscillatory Casson fluid flow in an annulus is a function of the frequency parameter, Schmidt number, fluctuating pressure component besides its dependency on time, annular gap and yield stress of the fluid. The mean concentration expression is derived in terms of these two coefficients. It is observed that the dispersion in oscillatory flow in Casson fluid flow inherently different from the steady flow, which is due to change in the plug flow region during the cycle of oscillations. It can be inferred that the decrease in annular gap inhibits the dispersion process, which could be due to decrease in annular gap leads to decrease in the flow and hence causes the lower mass transfer rate. It is observed that the dispersion coefficient decreases from 2.145×10^{-4} to 2.476×10^{-5} in the case Casson fluid ($\tau_y = 0.05$) from the case of tube to annulus with inner cylinder radius 0.1 i.e is about 88% of reduction in the dispersion coefficient. The results of this study are analysed to understand

the role played by the size of the catheter in a catheterized artery. It can be inferred that the presence of catheter and an increase in the catheter size inhibit the dispersion process.

References

1. R. Aris, *On the dispersion of a solute in a fluid flowing through a tube*, Proc. Roy. Soc. A **235** (1956), 67-77.
2. R. Aris, *On Dispersion of a Solute by Diffusion, Convection and Exchange between Plates*, Proc. Roy. Soc. A **252** (1959), 538-550 .
3. R. Aris, *On the dispersion of a solute in a pulsatile flow through a tube*, Proc. Roy. Soc. A **259** (1960), 370-376.
4. L.H. Back, *Estimated mean flow resistance increase during coronary artery catheterization*, J Biomech. **27** (1994), 169-175.
5. R.B. Bird, W.E. Stewart and E.N. Lightfoot, *Transport phenomena*, Wiley, New York, 1960.
6. G.F. Bloomingburg and G. Carta, *Separation of protein mixtures by continuous annular chromatography with step elution*, The Chemical Engineering journal and the Biochemical engineering journal **55** (1994), B19-B27.
7. W.E. Boyce and R.C. DiPrima,*Elementary differential equations and boundary value problems*, Wiley, New York, 2004.
8. C.G. Caro, T.J. Pedley, R.C. Schroter and W.A. Seed,*The mechanics of circulation*, Oxford University press, New York, 1978.
9. G. Carta, J.P. DeCarli, C.H. Byers and W.G. Sisson, *Separation of metals by continuous annular chromatography with step elusion*, Chemical Engineering Communications **79** (1989),207-227.
10. S. Charm and G. Kurland, *Viscometry of human blood for shear rates of 0-100,000 sec*$^{-1}$, Nature **206** (1965), 617-618.
11. P.C. Chatwin, *On the longitudinal dispersion of passive contaminant in oscillatory flow in tube*, J Fluid Mech. **7** (1975), 513-527.
12. C.J. Chen and H.C. Chen, *Finite analytic numerical method for unsteady two – dimensional Navier –Stokes equations*, J.Compt.Phys. **53** (1984), 209-226.
13. G.R. Cokelet, E.W. Merrill, E.R. Gilliland, H. Shin , A. Britten, and R.E. Wells, *The rheology of human blood measurement near andat zero shear rate*, Transactions of the Society of Rheology **7** (1963),303-317.
14. R.K. Dash, G. Jayaraman and K.N. Mehta, *Estimation of increased flow resistance in a narrow catheterized Artery-A theoretical model*, J. Biomechanics **29** (1996), 917 -930.
15. R.K. Dash, G. Jayaraman and K.N. Mehta, *Shear augmented dispersion of a solute in a Casson fluid flowing in a conduit*, Annals of Biomedical Engineering **28** (2000), 373-385.
16. J.P. DeCarli, *Displacement separations by continuous annular Chromatography*, AIChEJ, **36** (1990), 1220-1228.
17. Y.C. Fung, *Biomechanics: Mechanical properties of living tissues*,Springer Verlag, New York , 1993.
18. W.N. Gill and R. Sankarasubramanian, *Exact analysis of unsteady convective diffusion*, Proc. Roy. Soc. A **316** (1970), 341-350.
19. C.A. Goresky and M. Silverman, *Effect of correction of catheter distortion on calculated liver sinusoidal volumes*, Am.J.Physiol. **207** (1963), 883-892.
20. P.E. Hydon and T.J. Pedley, *Axial dispersion in a channel with oscillating walls*, J. Fluid Mech. **249** (1993), 535-555.
21. Y. Jiang and J.B. Grotberg, *Bolus contaminant dispersion in oscillatory tube flow with conductive walls,* J. of Biomech. Engg. Trans. ASME **115** (1993), 424-431.

22. D.A. McDonald, *Blood flow in arteries*, Edward Arnold, London,1974.
23. E.W. Merrill, E.R. Gilliland, G. Cokelet, H. Shin and A. Britten, R.E. Wells, *Rheology of human blood and flow in microcirculation*, Journal of Applied Physiology **18** (1963a), 255-260.
24. E.W. Merrill, E.R. Gilliland, G.R. Cokelet, H. Shin and A. Britten, R.E. Wells, *Rheology of human blood near and zero flow: effects of temperature and hamatocrit level.* Biophysical Journal. **3** (1963b),199-213.
25. E.W. Merrill, and G.A. Pelletier, *Viscosity of human blood: transition from Newtonian to non-Newtonian*, Journal of Applied Physiology, **23** (1967), 178-182.
26. W.R. Milnor and A. D. Jose, *Distortion of indicator-dilution by sampling systems*, J. Appl. Physiol. **15** (1960), 177-180.
27. P. Nagarani, G.Sarojamma and G. Jayaraman, *Effect of boundary absorption on dispersion in Casson fluid flow in an annulus - application to catheterized artery*, Acta Mechanica **202** (2009), 47-63.
28. D. Parrish, G.E. Gibbons and J.W. Bell, *A method for reducing the distortion produced by catheter sampling systems*, JAppl.Physiol. **17** (1962), 369-371.
29. T.J. Pedley and R.D. Kamm, *The effect of secondary motion on axial transport in oscillatory tube flow*, J. Fluid Mech. **193** (1988), 347-367.
30. B. Ramana and G. Sarojamma, *Effect of wall absorption on dispersionof a solute in a Herschel –Bulkley fluid through an annulus*, Advances in Applied Science Research. **3** (2012), 3878-3889.
31. R.A. Rao and K.S. Deshikachar, An exact analysis of unsteady convective diffusion in an annular pipe. Zeitschrift für Angewandte Mathematik und Mechanik (ZAMM) **67** (1987), 189-195.
32. A. Sarkar and G. Jayaraman, *The effect of wall absorption in annulus flow: Application to a catheterized artery*, Acta Mechanica **158** (2001),105-1119.
33. A. Sarkar and G. Jayaraman, *The effect of wall absorption on dispersion in an oscillatory flow in an annulus: Application to a catheterized artery*, Acta Mechanica **172** (2004), 151-167.
34. G. Sparacino, P. Vicini, R. Bonadonna, P. Marraccini, M. Lehtovitra, E. Ferrannini and C. Cobelli, *Removal of catheter distortion in multiple indicator dilution studies: a deconvolution- based method and case studies on glucose blood-tissue exchange,* Med Biol Eng Comput. **35** (1997), 337-42.
35. G.I. Taylor, *Dispersion of soluble matter in solvent flowing slowly through a tube*, Proc. Roy. Soc. A **219** (1953),186-203.
36. S. Tsangaris and N. Athanassiadis, *Diffusion in oscillatory flow in an annular pipe*, Zeitschrift Für Angewandte Mathematik Und Mechanik*(ZAMM)* **65** (1985), 252-254.

P. Nagarani got M.Sc, M.Phil and Ph.D from Sri Padmavati Women's University , Tirupati, Andhra Pradesh, India. She is presently in the position of Senior Lecturer at The University of the West Indies Mona Campus, Jamaica. Her research interests are Fluid Mechanics, Numerical methods for Partial differential Equations. Department of Mathematics,

University of the West Indies, Mona Campus Kingston, Jamaica
e-mail:nagarani_ponakala@yahoo.co.in

B.T. Sebastian received M.Sc. from Manglore University,India and Ph.D. at University of The West Indes. She is currently a lecturer at University of Technology, Jamaica. Her research interests are Fluid Mechanics and applicaton Partial differential Equations.

Department of Mathematics, Universty of Technology, Jamaica
e-mail: binil5@yahoo.com